# Eulerian–Lagrangian analysis of solid particle distribution in an internally heated and cooled air-filled cavity

F. Garoosi [a], M.R. Safaei [b], M. Dahari [c], K. Hooman [d,*]

[a] Department of Mechanical Engineering, University of Semnan, Semnan, Iran
[b] Young Researchers and Elite Club, Mashhad Branch, Islamic Azad University, Mashhad, Iran
[c] Department of Mechanical Engineering, Faculty of Engineering, University of Malaya, 50603 Kuala Lumpur, Malaysia
[d] School of Mechanical and Mining Engineering, The University of Queensland, Qld 4072, Australia

ARTICLE INFO

*Keywords:*
Natural convection
Eulerian–Lagrangian method
Thermophoresis
Heater
Cooler

ABSTRACT

A parametric study has been conducted to investigate particle deposition on solid surfaces during free convection flow in an internally heated and cooled square cavity filled with air. The cavity walls are insulated while several pairs of heaters and coolers (HACs) inside the cavity lead to free convection flow. The HACs are assumed to be isothermal heat source and sinks with temperatures $T_h$ and $T_c$ ($T_h > T_c$). The problem is numerically investigated using the Eulerian–Lagrangian method. Two-dimensional Navier–Stokes and energy equations are solved using finite volume discretization method. Applying the Lagrangian approach, 5000 particles, distributed randomly in the enclosure, were tracked for 150 s. Effects of drag, lift, gravity, buoyancy, pressure gradient, shear stress terms, thermophoresis and Brownian forces on particles movements are considered. Furthermore, effects of various design parameters on the heat transfer rate and deposition of particles such as Rayleigh number ($10^4 \leqslant Ra \leqslant 10^7$) as well as orientation and number of the HACs are investigated. Our simulations indicate that thermophoretic force can significantly affect the distribution of particles of $d_p = 1$ μm diameter. It is also found that at low Rayleigh numbers the particle distribution is strongly non-uniform. Moreover, it was observed that by increasing number of the HACs and changing orientation of the HACs from vertical to horizontal, deposition rate of the solid particles increases significantly.



## 1. Introduction

Natural convection fluid flow and heat transfer in enclosed spaces with a heater and/or cooler inside are encountered in a number of industrial applications such as indoor ventilation with radiators, cooling of electrical components, and heat exchangers [1]. From energy saving point of view, improvement of heat transfer in any application of natural convection is a primary and crucial topic. Thus, several investigations can be found concentrating on natural convection [2–7]. Deng [2] studied laminar natural convection in a two dimensional square enclosure with two and three source–sink pairs on the vertical side walls. Park et al. [3] investigated and reported natural convection in a square cavity with two hot inner circular cylinders at different vertical locations. They highlighted that heat transfer rate has a direct relationship with Rayleigh number. Saravanan et al. [6] performed a numerical study of natural convection in a differentially heated square

* Corresponding author.
*E-mail address:* k.hooman@uq.edu.au (K. Hooman).

http://dx.doi.org/10.1016/j.amc.2014.10.068
0096-3003/

**Nomenclature**

| | |
|---|---|
| $A$ | dimensionless surface area per depth $A = 2(L + W)$, m |
| $C_c$ | Cunningham's factor |
| $C_D$ | drag coefficient |
| $C_m$ | constant in Eq. (17) (=1.14) |
| $C_p$ | specific heat, J kg$^{-1}$ K$^{-1}$ |
| $C_s$ | constant in Eq. (17) (=1.17) |
| $C_t$ | constant in Eq. (17) (=2.18) |
| $d_p$ | diameter of the nanoparticle, m |
| $d_{ij}$ | deformation tensor $= (u_{i,j} + u_{j,i})/2$ |
| $F_{L,i}$ | lift force per unit mass in the $i$ direction, ms$^{-2}$ |
| $F_{Th,i}$ | thermophoretic force per unit mass in the $i$ direction, ms$^{-2}$ |
| $F_B$ | Brownian force per unit mass in the $i$ direction, ms$^{-2}$ |
| $F_{P,i}$ | pressure gradient force per unit mass in the $i$ direction, ms$^{-2}$ |
| $F_{\mu,i}$ | shear stress per unit mass in the $i$ direction, ms$^{-2}$ |
| $g$ | gravity acceleration, ms$^{-2}$ |
| $G_i$ | Gaussian random numbers |
| $H$ | enclosure height, m |
| $L$ | dimensional height of the heater and cooler, m |
| $K$ | constant in Eq. (14) (=2.594) |
| $k_B$ | Boltzmann constant (=$1.38 \times 10^{-23}$) |
| $k$ | fluid thermal conductivity, Wm$^{-1}$ K$^{-1}$ |
| $k_p$ | particle thermal conductivity, Wm$^{-1}$ K$^{-1}$ |
| $Kn$ | Knudsen number (=$2\lambda/d$) |
| $N$ | number of particles or pairs of the HACs |
| $\overline{Nu}_i$ | average Nusselt number on the walls of $i$th heater |
| $p$ | fluid pressure, ($Pa$), N m$^{-2}$ |
| $Pr$ | Prandtl number ($= \nu_f/\alpha_f$) |
| $R$ | universal gas constant, J K$^{-1}$ mol$^{-1}$ |
| $Ra$ | Rayleigh number $= g\beta_f(T_h - T_c)H^3/\alpha_f\nu_f$ |
| $\mathrm{Re}_p$ | relative Reynolds number (=$\rho d_p\|u_p - u\|/\mu$) |
| $S$ | relative density (=$\rho_p/\rho$) |
| $St$ | Stokes number |
| $T$ | fluid temperature, K |
| $T_0$ | reference temperature (=$(T_h + T_c)/2$), K |
| $t$ | time, s |
| $u$, $v$ | dimensional velocity components, ms$^{-1}$ |
| $u_i$ | fluid velocity in the $i$ direction, ms$^{-1}$ |
| $u_{p,i}$ | particle velocity in the $i$ direction, ms$^{-1}$ |
| $x$, $y$ | dimensional Cartesian coordinates, m |
| $X$, $Y$ | dimensionless Cartesian coordinates, m |

*Greek symbols*

| | |
|---|---|
| $\rho$ | density, kg m$^{-3}$ |
| $\beta$ | thermal expansion coefficient, K$^{-1}$ |
| $\theta$ | dimensionless temperature |
| $\mu$ | dynamic viscosity, kg m$^{-1}$ s$^{-1}$ |
| $\nu$ | kinematic viscosity, m$^2$s$^{-1}$ |
| $\tau$ | particle relaxation time (Eq. (10)), s |
| $\alpha$ | thermal diffusivity, m$^2$s |
| $\nabla$ | gradient |
| $\Delta$ | delta |

*Subscripts*

| | |
|---|---|
| $c$ | cold or cooler |
| $f$ | base fluid |
| $h$ | hot or heater |
| $i$ | vector axis indicators |
| $L$ | lift |
| $p$ | particle |
| $Th$ | thermophoresis |
| $B$ | Brownian |

(DHC) cavity containing two vertical thin heaters. They found that by changing location of the two vertical thin heaters, the heat transfer rate inside the cavity changes significantly.

On the other hand, particulate fouling, i.e. particle deposition on heat exchanger surfaces can reduce the heat transfer rate and adversely affect the energy efficiency of these equipment [8,9]. Therefore, several studies have been carried out to understand this problem using Eulerian–Lagrangian methods [10–27].

Akbar et al. [11] focused on the effects of thermophoresis and Brownian motion in natural convection for solid particles with diameters in the range of 50 nm to 1 μm. Their results show that random pattern of particle deposition is a result of Brownian motion which is more pronounced in case of submicron size particles. In addition, according to those authors by increasing the Rayleigh number the effects of Brownian motion becomes weaker and particle deposition rate decreases. Bagheri et al. [12] numerically simulated the deposition of solid particles with diameters between 10 nm and 10 μm in a differentially heated cavity filled with air. It was reported that the effects of thermophoretic and Brownian force are important on the distribution and deposition of sub-micron particles. Moreover, their results show that trapping of particles in the recirculation zone decreases the deposition rate. Golkarfard et al. [14] investigated laminar mixed convection in a two-dimensional lid-driven cavity with two heaters attached to the bottom wall of the cavity to note that particle deposition rate increases significantly by either increasing the heater size or the spacing between the heaters. He et al. [16] investigated deposition of aerosol particles in duct flows including the effect of thermal force under laminar and turbulent flow. They found that in laminar regime for particles with $0.1 \leqslant d_p \leqslant 1$ μm, the thermophoretic force becomes the dominant transport mechanism and controls the particle deposition rate. Li et al. [18] worked on the effects of thermophoresis and Brownian force in a turbulent channel flow to note that Brownian force significantly affects the dispersion of small particles with $d_p \leqslant 50$ nm while for particles larger than 1 μm the deposition rate increases rapidly with particle size. Puragliesi et al. [20] studied the effects of solid particle diameter on their flow patterns in a differentially heated cavity (DHC) to observe that by increasing the particle diameter to 10 μm the effect of gravitational forces becomes more important and therefore most of the depositions occurred on the bottom wall. Saidi et al. [21] and Vegendla et al. [22] studied the behavior of solid particles by using Eulerian–Lagrangian and Eulerian–Eulerian method for dilute gas–solid flow. They found that the Eulerian–Lagrangian method is more accurate than Eulerian–Eulerian method. Wang et al. [23] applied the detached eddy simulation method to study the behavior of the solid particle in enclosed spaces. According to those authors, the distribution of particle deposition onto surfaces depends on particle size and the airflow pattern in the cabin. Meanwhile, their results indicate that 35% of the small particles (700 nm), 55% of the medium particles (10 μm), and 100% of the large particles (100 μm) deposited onto the cabin surface and the rest were removed by the cabin ventilation.

In view of the above, a comprehensive study investigating the effects of different forces on particle flow and deposition on solid surfaces as a result of buoyancy-induced flow, caused by internal heating and cooling in a cavity, is missing in the literature. Hence, on top of addressing this question, the effects of design parameters, e.g. the orientation and number of HACs, on the rate of heat transfer and the deposition of particles inside the cavity will be investigated in this work. For this purpose, motion of 5000 particles, over a wide range of particle sizes, is investigated numerically using an Eulerian–Lagrangian solver.

## 2. Problem statement

As depicted by Fig. 1, a square air-filled cavity of size, $H$, is considered where all cavity walls are insulated. Heat is generated internally through isothermal heat sources. This generated heat is then transferred to internal isothermal heat sinks of identical size and shape. These pairs of heaters and coolers (HACs) are creating local temperature gradients as a result of which the air density changes and free convection instabilities kick in. Commensurate with that, heat is convected away from the sources and is transferred to adjacent heat sinks. HACs are rectangular in shape with dimensionless width and length of $W$ and $L$, respectively. Surface area per unit depth of each source or sink is equal to $A = 2(L + W)$. We have assumed fixed surface temperatures for heaters and coolers, i.e. $T_h = 273$ K and $T_c = 373$ K ($\Delta T = 100$ K). Similar to [28], the thermophysical properties of the base fluid (air) and solid particles in this study are evaluated at the average fluid temperature $(T_h + T_c)/2$ as per Table 1. Assumptions for the simulation are as follows:

- Newtonian fluid and two-dimensional flow,
- Thermophysical properties are constant except for the air density which varies according to the Boussinesq approximation,
- Following [10,11,29], it is assumed that for such low volume fractions of solid particles considered here the particles have negligible effects on the flow field,
- The initially stagnant particles are distributed randomly in the cavity,
- Local thermal equilibrium between the particle and air,
- Particles are sticky, i.e. they will stick to the surface when they come in contact with the walls [15,19].

## 3. Mathematical formulation

The two-dimensional transient equations of the continuity, momentum and energy for an incompressible flow are given by:

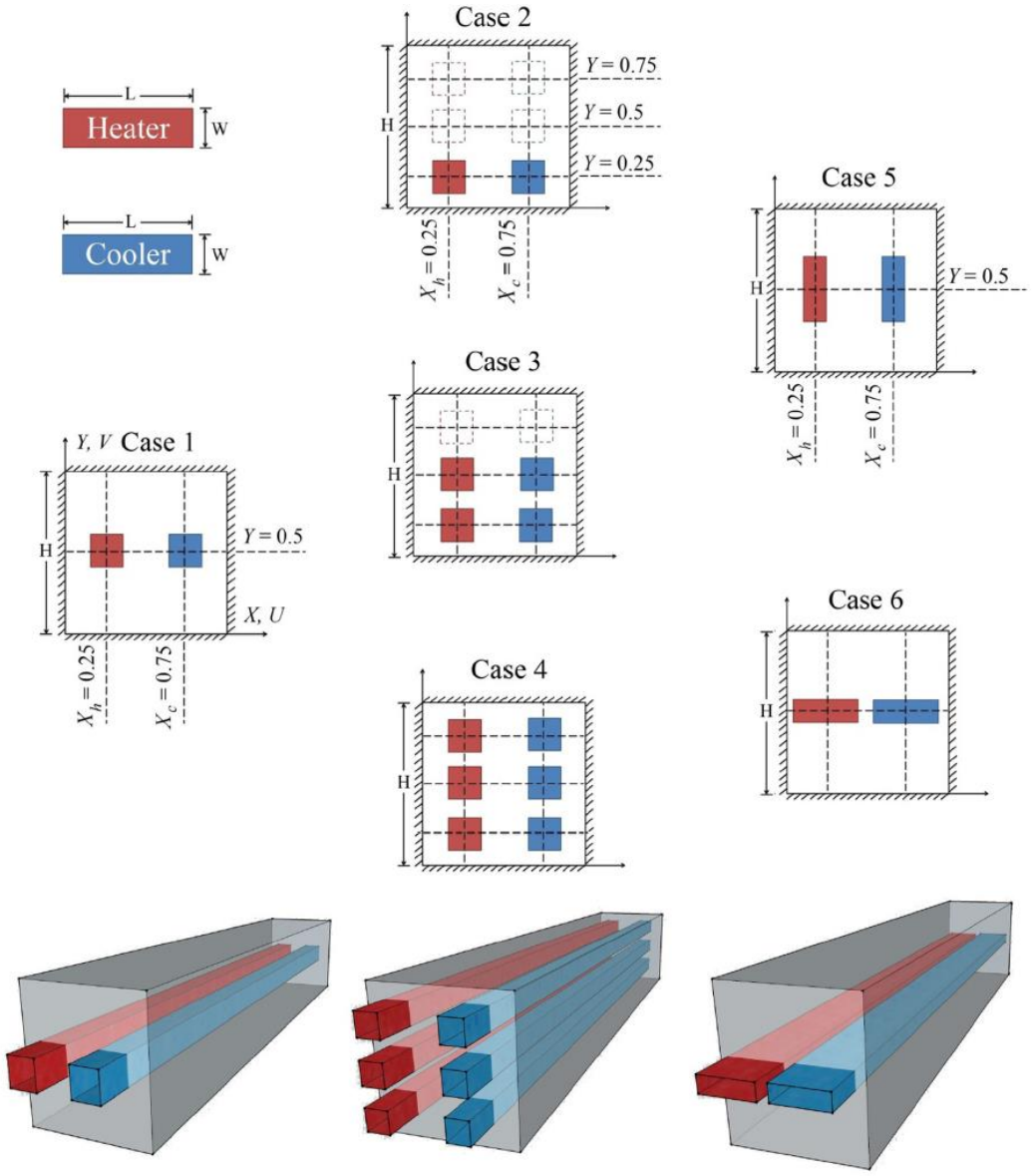


**Fig. 1.** Schematic of the square cavity (heat exchanger) with the HAC(s). Location of the HAC for each case is shown by dashed line.

**Table 1**
Thermo-physical properties of the base fluid (*Air*) and solid particles [28].

| | $\rho$ (kg/m$^3$) | K (W/m K | $C_p$ (j/kg K) | $\beta \times 10^5$ (K$^{-1}$) | $\mu \times 10^7$ (kg m$^{-1}$ s$^{-1}$) | *Pr* |
|---|---|---|---|---|---|---|
| Air | 1.085 | 0.028 | 1007 | 308.64 | 196.4 | 0.703 |
| Solid particle | 2220 | 1.38 | 745 | ———— | ———— | ——— |

### 3.1. Fluid and thermal field

$$\frac{\partial u}{\partial x}+\frac{\partial v}{\partial y}=0, \tag{1}$$

$$\frac{\partial u}{\partial t}+u\frac{\partial u}{\partial x}+v\frac{\partial u}{\partial y}=-\frac{1}{\rho_f}\frac{\partial p}{\partial x}+\frac{\mu_f}{\rho_f}\left(\frac{\partial^2 u}{\partial x^2}+\frac{\partial^2 u}{\partial y^2}\right), \tag{2}$$

$$\frac{\partial v}{\partial t}+u\frac{\partial v}{\partial x}+v\frac{\partial v}{\partial y}=-\frac{1}{\rho_f}\frac{\partial p}{\partial y}+\frac{\mu_f}{\rho_f}\left(\frac{\partial^2 v}{\partial x^2}+\frac{\partial^2 v}{\partial y^2}\right)+g\beta_f(T-T_c), \tag{3}$$

$$\frac{\partial T}{\partial t}+u\frac{\partial T}{\partial x}+v\frac{\partial T}{\partial y}=\alpha_f\left(\frac{\partial^2 T}{\partial x^2}+\frac{\partial^2 T}{\partial y^2}\right), \tag{4}$$

The corresponding boundary and initial conditions are:

$$\begin{aligned} &u=v=0,\ \tfrac{\partial T}{\partial n}=0 && \text{on cavity walls,}\\ &u=v=0,\ T=T_h && \text{on heater walls,}\\ &u=v=0,\ T=T_c && \text{on cooler walls,}\\ &u=v=u_p=v_p=0 && \text{initial conditions for fluid and solid particles at } t=0. \end{aligned} \tag{5}$$

The average Nusselt number for each isothermal heater is computed as:

$$\overline{Nu}_i=\frac{1}{L}\int_{X_h-\frac{L}{2}}^{X_h+\frac{L}{2}}\left\{\left.\frac{\partial\theta}{\partial Y}\right|_{bottom}+\left.\frac{\partial\theta}{\partial Y}\right|_{upper}\right\}dX+\frac{1}{W}\int_{Y_h-\frac{W}{2}}^{Y_h+\frac{W}{2}}\left\{\left.\frac{\partial\theta}{\partial X}\right|_{left}+\left.\frac{\partial\theta}{\partial X}\right|_{right}\right\}dY, \tag{6}$$

and the total Nusselt number is defined by adding $\overline{Nu}_i$ values of all heaters divided by number of heaters:

$$Nu_{tot}=\sum_{i=1}^{N}\overline{Nu}_i/N. \tag{7}$$

### 3.2. Particle equation of motion

The equations of particle dispersion are given as [12,24]:

$$\frac{du_{p,i}}{dt}=F_{D,i}+F_{L,i}+F_{G,i}+F_{P,i}+F_{\mu,i}+F_{B,i}+F_{Th,i}, \tag{8}$$

$$\frac{dx_{p,i}}{dt}=u_{p,i}. \tag{9}$$

The left hand side of Eq. (8) represents the inertial force per unit mass, where $F_{D,i}$ is the drag force (per unit mass) defined as:

$$F_{D,i}=\frac{C_D\mathrm{Re}_p}{24\tau}(u_i-u_{p,i}). \tag{10}$$

The drag coefficient is a function of particle Reynolds number, $\mathrm{Re}_p=\frac{\rho_f d_p|u_p-u_f|}{\mu_f}$, for spherical particles and is given as:

$$\begin{cases} C_D=\frac{24}{\mathrm{Re}_p} & \mathrm{Re}_p<1,\\ C_D=\frac{24}{\mathrm{Re}_p}\left(1+\frac{\mathrm{Re}_p^{2/3}}{6}\right) & 1<\mathrm{Re}_p<1000,\\ C_D=0.44 & \mathrm{Re}_p>1000. \end{cases} \tag{11}$$

**Table 2**
Effect of the grid size on $Nu_{tot}$. Square enclosure filled with air ($Pr=0.703$) with three pairs of heaters and coolers, $L=W=0.15H$ (case 4).

| *Ra* | Grid size | | | | | | |
|---|---|---|---|---|---|---|---|
| | 49 × 49 | 69 × 69 | 89 × 89 | 109 × 109 | 129 × 129 | **149 × 149** | 169 × 169 |
| $10^4$ | 1.071571 | 1.081197 | 1.088483 | 1.094394 | 1.095939 | 1.096455 | 1.096939 |
| $10^7$ | 10.07682 | 10.09539 | 10.11004 | 10.12373 | 10.12722 | 10.12774 | 10.12847 |

In Eq. (10), $\tau$ is the relaxation time defined as:

$$\tau = \frac{Sd_p^2 C_c}{18\upsilon}, \tag{12}$$

where $C_c$ is the Cunningham correction factor given by:

$$C_c = 1 + \frac{2\lambda}{d}\left(1.257 + 0.4e^{-1.1d_p/2\lambda}\right). \tag{13}$$

$F_{L,i}$ is the shear-induced lift force (per unit mass) which is based on the model of Li and Ahmadi [18]; a generalization of the expression provided by Saffman [30]:

$$F_{L,i} = \frac{2K\upsilon^{0.5}\rho d_{ij}}{\rho_p d_p (d_{lk}d_{kl})(u - u_{p,i})}, \quad d_{ij} = \frac{1}{2}(u_{i,j} + u_{j,i}). \tag{14}$$

Here, $K = 2.594$ is the constant in Saffman's lift force, and $d_{ij}$ is the deformation rate tensor.

$F_{G,i}$ (buoyancy force per unit mass), $F_{P,i}$ (fluid pressure gradient per unit mass) and $F_{\mu,i}$ (shear stress per unit mass) in Eq. (8) can be calculated as:

$$F_{G,i} = \frac{g_i(\rho_p - \rho_f)}{\rho_p}, \quad F_{P,i} = -\frac{1}{\rho_p}\nabla P, \quad F_{\mu,i} = \frac{\mu_f}{\rho_p}\nabla^2 \vec{U}, \tag{15}$$

In Eq. (8), $F_{B,i}$ represents the stochastic excitation due to the Brownian motion:

$$F_{B,i} = Gi \times \sqrt{\frac{216}{\pi}\frac{\upsilon k_B}{\rho_f d_p^5 S^2 C_c}\frac{T}{\Delta t}}, \tag{16}$$

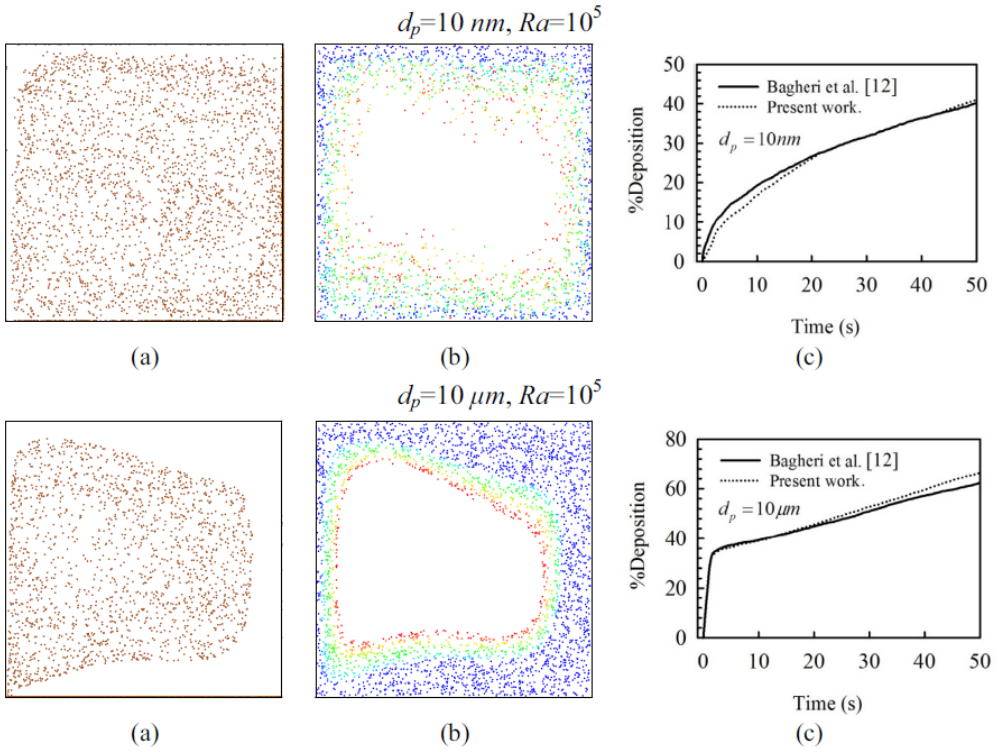


**Fig. 2.** Validation for Lagrangian part of the code, partially heated hot wall filled with air ($Pr = 0.71$). (a) Locations of the particles after 50 s; (b) initial location of deposited particles in the cavity. Color indicates the deposition time in seconds; (c) comparison of time variation of %deposition obtained in the present study and Bagheri et al. [12]. (For interpretation of the references to color in this figure legend, the reader is referred to the web version of this article.)

The last term, $F_{Th}$ stands for thermophoretic force which is evaluated using the expression suggested by Talbot et al. [31]:

$$F_{Th,i} = \frac{-36\mu^2 C_s(k/k_p + C_t + Kn)}{\rho_f \rho_p d_p^2 (1 + 3C_m Kn)(1 + 2k/k_p + 2C_t Kn)} \frac{\nabla T}{T}. \tag{17}$$

Here, $k$ and $k_p$ are the thermal conductivities of air and solid particle, respectively, and $C_m = 1.14$, $C_t = 2.18$, and $C_s = 1.17$.

## 4. Numerical implementation

The dimensional governing equations (Eqs. (1)–(4)) along with the boundary and conditions described by Eq. (5) are discretized using finite volume method [32] on a staggered grid. SIMPLE algorithm is used for implicit pressure–velocity coupling while hybrid differencing scheme of Spalding [33] is used for the convective terms. The resulting equation systems were solved in each time step using the line-by-line method (TDMA) [32] until the steady state is reached (sum of residuals became less than $10^{-7}$). Particles are then introduced to the computational domain. Hence, applying the Lagrangian method, Eqs. (8) and (9) governing the particles dispersion are solved. Moving from ensembles of 1000 to 30,000 particles lead to no significant change in the results. Therefore, ensembles of 5000 particles with random initial positions and zero initial velocities were tracked over 150 s at different $Ra$ for case 1 to 6. Numerical calculations were performed by writing a computer program in FORTRAN.

### 4.1. Grid independence

In order to find the proper grid size for the numerical implementation, free convection in a cavity filled with air ($Pr = 0.703$) including three pairs of HACs (see Fig. 1, case 4) with the size of $L = W = 0.15H$ is simulated at two extreme Rayleigh numbers ($Ra = 10^4$ and $10^7$). $Nu_{tot}$ is calculated using seven different uniform grids (spatial and temporal pairs) and results are presented in Table 2. Fixing the 149 × 149 spatial grids, $Nu_{tot}$ results are found to be independent of grids, as Table 2 shows, when finer girds are selected. The time step $dt$ is set at $10^{-4}$ s in all the particle transport calculations. The effect of time step on the deposition rate of the solid particles was tested by repeating some of the calculations with shorter time steps, and was found to be small enough (based on their relaxation time) to be neglected.

### 4.2. Code verification

Our results are verified against those of Bagheri et al. [12] pertinent to modeling solid particles of diameters between 10 nm and 10 μm in a differentially heated cavity filled with air. Fig. 2a shows a comparison between our results and those

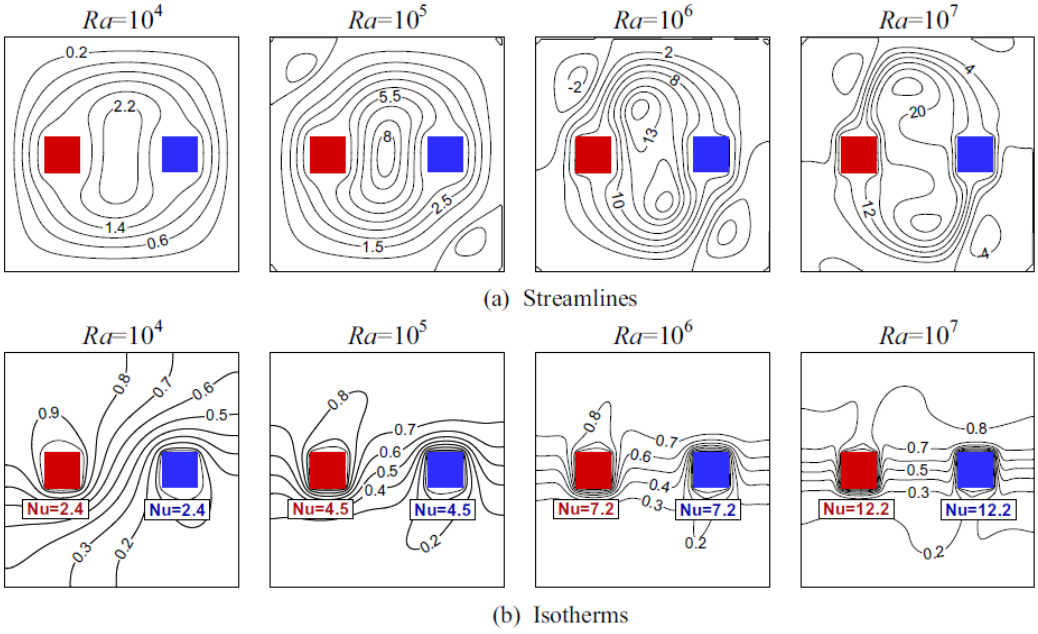


**Fig. 3.** (a) Streamlines and (b) isotherms inside the square enclosure filled with air ($Pr = 0.7$) at different Rayleigh numbers for case 1 ($L = W = 0.15H$).

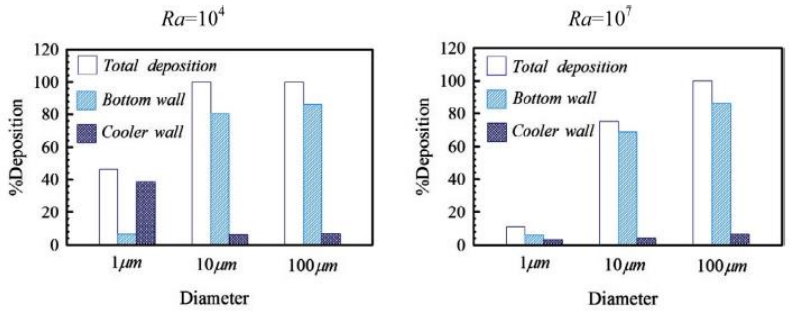


**Fig. 4.** The effects of particles diameter on deposition of the solid particles at two different Rayleigh numbers for case 1 ($L = W = 0.15H$).

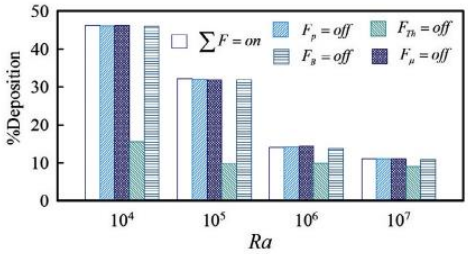


**Fig. 5.** Particle deposition in the absence and presence of forces for case 1 after 2.5 min of tracking ($t = 150$ s).

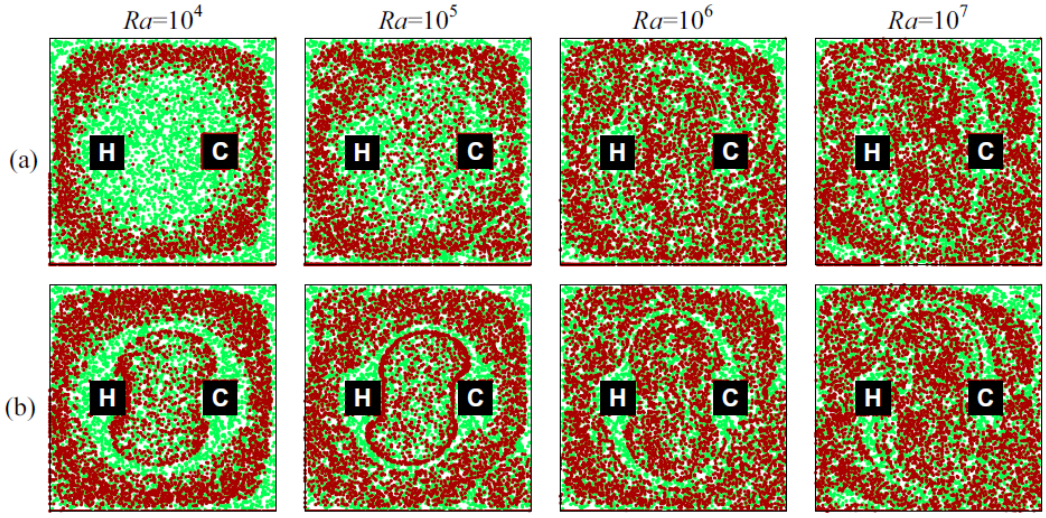


**Fig. 6.** Distribution of the solid particles in the absence and presence of thermophoresis for particle diameters of 1 μm in case 1. The green color indicates initial position of particles ($t = 0$) and the red color indicates location of the particles after 2.5 min of tracking; (a) $F_{Th} = on$ and (b) $F_{Th} = off$. (For interpretation of the references to color in this figure legend, the reader is referred to the web version of this article.)

of Bagheri et al. [12] for extreme particle sizes of 10 nm and 10 μm after 50 s. Fig. 2b shows initial position of particles deposited on the cavity walls after 50 s. Finally, Fig. 2c shows comparisons of particle deposition between this study and results of Bagheri et al. [12] for particle diameters of 10 nm and 10 μm at $Ra = 10^5$. A close agreement is observed.

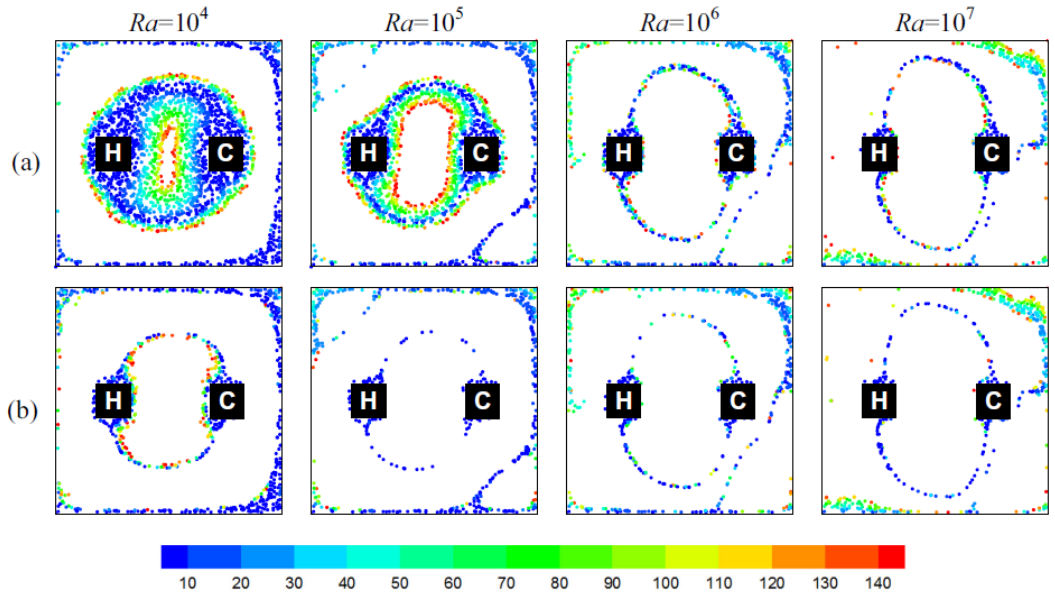


**Fig. 7.** The initial location of the particles which after 2.5 min of tracking, have been deposited in the cavity. Color indicates the deposition time in second; (a) $F_{Th} = on$ and (b) $F_{Th} = off$. (For interpretation of the references to color in this figure legend, the reader is referred to the web version of this article.)

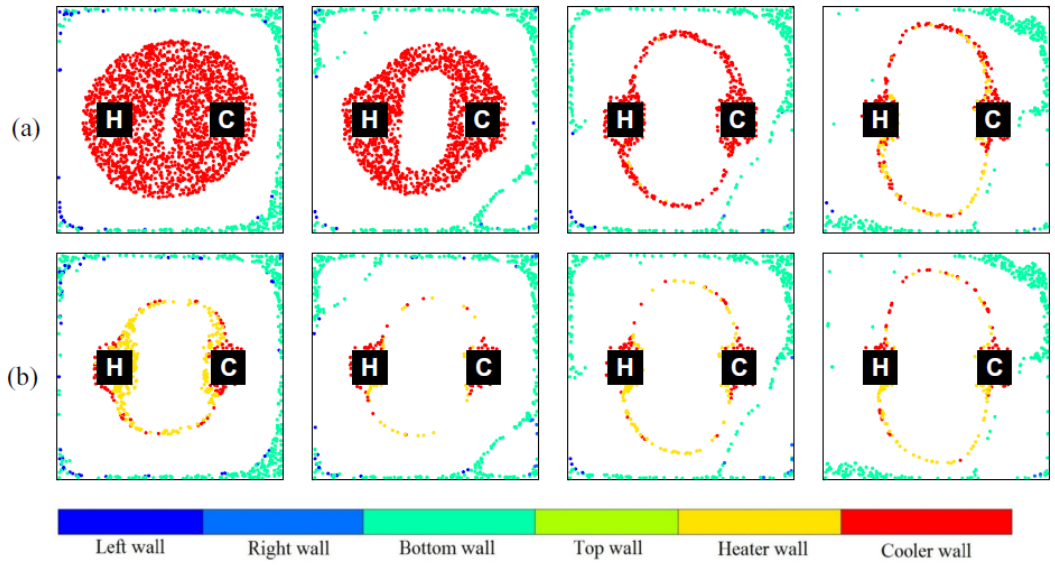


**Fig. 8.** The initial location of the particles which after 2.5 min of tracking, have been deposited in the cavity. The colors indicate the location of particle deposition on one of the walls of the cavity, heater or cooler; (a) $F_{Th} = on$ and (b) $F_{Th} = off$. (For interpretation of the references to color in this figure legend, the reader is referred to the web version of this article.)

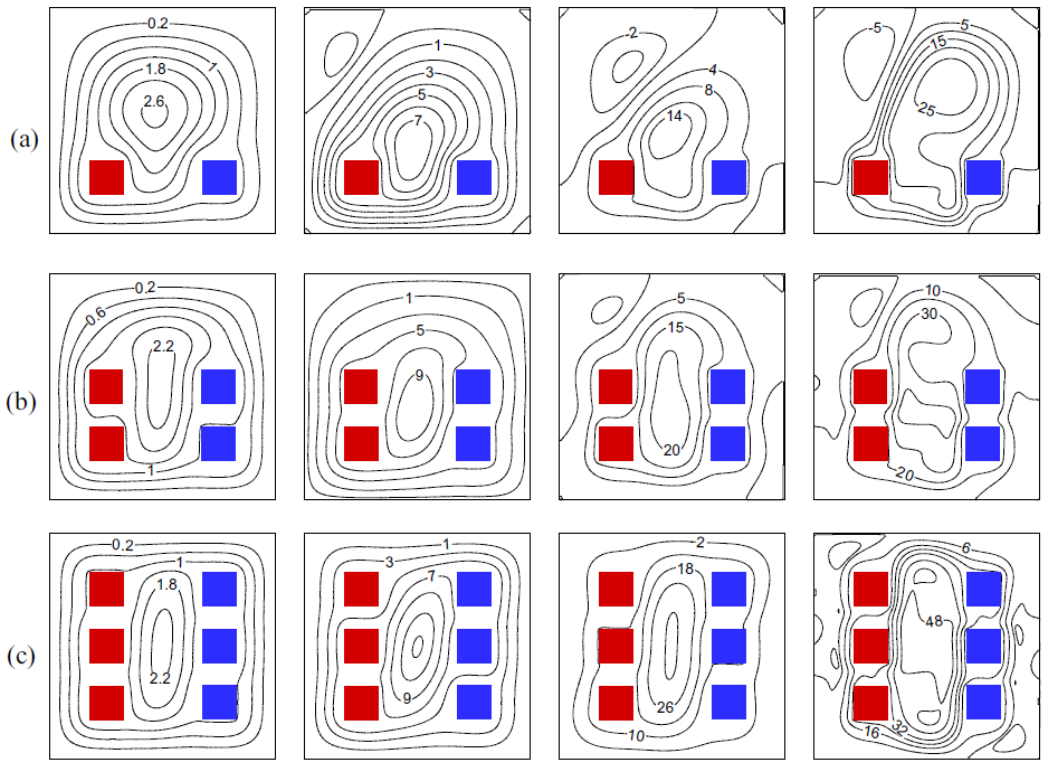


**Fig. 9.** Streamlines inside the square cavity filled with air ($Pr = 0.7$) at different Rayleigh numbers; (a) case 2, (b) case 3 and (c) case 4. $L = W = 0.15H$.

## 5. Results and discussion

Distribution of the solid particles in a square enclosure with several pairs of HACs is investigated through Eulerian–Lagrangian numerical simulations. Effects of various design parameters such as: orientation and numbers of HACs are studied. The effects of some other major parameters such as fluid pressure gradient, shear stress terms, thermophoretic force and Brownian motion on distribution of the solid particles are also investigated. For each combination, Rayleigh number is altered between $10^4$ and $10^7$.

### *5.1. The effects of particles diameters*

In this section, a square cavity filled with air containing a pair of HAC with $W = L = 0.15H$ is considered for heat transfer analysis and behavior solid particles at different *Ra* and particles diameters. Fig. 3(a and b) illustrate streamlines and isotherms for case 1 at various *Ra*. Fig. 3(a) shows that at low *Ra* a clockwise vortex forms within the cavity. By increasing Rayleigh numbers (and therefore the buoyancy force) to $Ra = 10^5$ and $10^6$, the intensity of the main vortex increases and two other small counterclockwise vortexes form near cavity corners. With further increase in *Ra* to $10^7$ the central vortex breaks into two cores and the shape of the central vortex core changes dramatically. Isotherms in Fig. 3(b) show that at low *Ra*, the heat transfer inside the cavity is mainly through conduction. With increase in the Rayleigh number, the effect of convection heat transfer becomes more significant and the isotherms get densely packed adjacent to the walls of heater and cooler (HAC).

Ensembles of 5000 particles with random spatial distributions were tracked over 150 s for different diameters of the solid particles at $Ra = 10^4$ and $10^7$. As Fig. 4 shows with an increase in the particle diameter from 1 to 100 μm, particle deposition rate increases significantly. It is due to the fact that by increasing the particle diameter from 1 to 100 μm the effect of gravity force becomes more important causing significant deposition on the bottom wall. This is in agreement with the findings of Puragliesi et al. [20] and Wang et al. [23], who reported that particles with $d_p \geqslant 10$ μm mostly deposit on the bottom wall of the enclosure. Hence, we only focus on the behavior of particles with $d_p = 1$ μm. In order to better understand the dispersion of particles, streamlines, isotherms and solid particle distribution of all cases considered in this study are shown.

***Link to Full-Text Articles :***

***http://www.sciencedirect.com/science/article/pii/S009630031401443X***

***www.researchgate.net/profile/Mohammad_Reza_Safaei/publication/268315542_Eulerian-Lagrangian_analysis_of_solid_particle_distribution_in_an_internally_heated_and_cooled_air-filled_cavity/links/54686fb60cf20dedafcf6186.pdf***